Canadian Science Publishing

ARTICLE

Atmospheric aerosols elevated ecosystem productivity of a poplar plantation in Beijing, China

Yuan Gao, Zhiqiang Zhang, Jiquan Chen, Steven McNulty, Hang Xu, Lixin Chen, Zuosinan Chen, and Zhihua Jin

Abstract: Atmospheric aerosols can influence energy allocation, environmental factors, and thus, canopy photosynthesis. However, the regulations of aerosols on ecosystem productivity are not well understood. Here, we applied the optical properties of aerosols to quantify the effects of aerosol type and concentration on the environmental factors and associated gross primary productivity (GPP) of a poplar (*Populus euramericana*) plantation during the months of June to August from 2014 to 2016 in Beijing, China. As aerosol optical depth (AOD) increased from 0 to 2.5, total photosynthetically active radiation (PAR) decreased by 29%, while the diffuse PAR increased by 39%. Although there was no significant impact of aerosols on air temperature ($p > 0.05$), aerosols decreased vapor pressure deficit by more than 40%. We found that the plantation GPP changed exponentially with AOD, indicating that aerosols elevated GPP by about 37% under severe aerosol pollution (AOD ≥ 1) compared with background aerosol (AOD < 0.4). Aerosols type also had a significant effect on GPP. We concluded that aerosols could increase the GPP of the poplar plantation, and the promotion effect of aerosols on poplar plantation would not be significantly reduced until AOD was <1 under the projected decrease in aerosol loading in the future.

Key words: aerosol, gross primary productivity, diffuse fertilization effect, environmental perturbation, poplar plantation.

Résumé : Les aérosols atmosphériques peuvent influencer la répartition de l'énergie, les facteurs environnementaux et, par conséquent, la photosynthèse du couvert forestier. Cependant, la régulation de l'effet des aérosols sur la productivité des écosystèmes n'est pas bien comprise. Dans cet article, nous avons appliqué les propriétés optiques des aérosols pour quantifier les effets du type et de la concentration des aérosols sur les facteurs environnementaux et la production primaire brute (PPB) d'une plantation de peuplier (*Populus euramericana*) durant les mois de juin et août, de 2014 à 2016 à Pékin en Chine. À mesure que la profondeur optique des aérosols (AOD) augmentait de 0 à 2,5, le rayonnement photosynthétiquement actif (RPA) total diminuait de 29 % tandis que le RPA diffus augmentait de 39 %. Malgré le fait que les aérosols n'aient pas eu d'impact significatif sur la température de l'air ($p > 0,05$), ils réduisaient le déficit de saturation de plus de 40 %. Nous avons trouvé que la PPB de la plantation changeait de façon exponentielle en fonction de l'AOD, indiquant que les aérosols augmentaient la PPB d'environ 37 % lorsque la pollution causée par les aérosols était sévère (AOD ≥ 1) comparativement à la concentration de base des aérosols (AOD $< 0,4$). Le type d'aérosols avait également un effet significatif sur la PPB. Nous concluons que les aérosols pourraient augmenter la PPB de la plantation et que l'effet stimulant des aérosols sur la plantation de peuplier ne diminuera pas de façon significative tant que la valeur de l'AOC ne deviendra pas inférieure à un en raison d'une diminution prévue de la charge des aérosols dans le futur. [Traduit par la Rédaction]

Mots-clés : aérosols, production primaire brute, effet diffus de fertilisation, perturbation environnementale, plantation de peuplier.

1. Introduction

Atmospheric aerosols directly affect the light-use efficiency (LUE) and ecosystem productivity by changing solar radiation and other microclimatic conditions (Kanniah et al. 2012; Mercado et al. 2009). At the ecosystem level, the effects of aerosols on the terrestrial ecosystem productivity have been reported as positive, negative, or neutral (Table 1). Enhanced diffuse radiation and the diffuse fraction due to aerosols can lead to higher LUE for complex canopies (Alton 2008; Alton et al. 2007), known as the diffuse fertilization effect (DFE) (Gu et al. 2002; Yue and Unger 2017). For example, there was an 8%–23% enhancement for the noontime gross photosynthesis of a northern hardwood forest in 2 years after the Mt. Pinatubo eruption under cloudless conditions (Gu et al. 2003). On the contrary, the negative effect of aerosols lies in the reduced total radiation for plants to sequestrating atmosphere carbon (Cohan et al. 2002; Oliveira et al. 2007). For example, when aerosol loading (i.e., aerosol optical depth, AOD) exceeded 2.7, ecosystem productivity of the forests in the Romanian region of Brazil was reduced to zero (Oliveira et al. 2007). The neutral

Received 12 September 2020. Accepted 29 January 2021.

Y. Gao, Z. Zhang, H. Xu, L. Chen, Z. Chen, and Z. Jin. Key Laboratory of Soil and Water Conservation & Desertification Combating, State Forestry and Grassland Administration, Beijing 100083, P.R. China; School of Soil and Water Conservation, Beijing Forestry University, Qinghua East Road 35, Haidian District, Beijing 100083, P.R. China.

J. Chen. Landscape Ecology & Ecosystem Science (LEES) Lab, Center for Global Change and Earth Observations (CGCEO), and Department of Geography, Michigan State University, East Lansing, MI 48823, USA.

S. McNulty. USDA Southeast Regional Climate Hub, 920 Main Campus Drive, Venture Center 2, Suite 300, Raleigh, NC 27606, USA.

Corresponding author: Zhiqiang Zhang (email: zhqzhang@bjfu.edu.cn).

Table 1. Summary of the aerosol effect on terrestrial ecosystem productivity studies.

Site	PFTs*	Latitude, longitude	AOD	Type†	Results‡	Reference
Blodgett Forest (California, USA)	ENF	38°53′N, 120°37′W	—	UI	Aerosols caused forest NEE to increase by 8%.	Misson et al. 2005
Morgan Monroe (Indiana, USA)	Varied	39°18′N, 86°24′W	0–0.9	UI	High AOD conditions enhanced plant productivity by ~13%.	Strada et al. 2015
Howard Springs (Darwin, Australia)	Savanna	12°30′S, 131°25′E	0–0.4	BB	Aerosol was negatively (but non-significantly) related to GPP.	Kanniah et al. 2010
K34 LBA tower (Manaus, Brazil)	EBF	2°36′S, 60°12′W	0–0.7	BB	NEE increased by 20%, when AOD ranged from 0.1 to 0.7.	Cirino et al. 2014
FLONA-83 (Floresta, Brazil)	EBF	3°01′S, 54°59′W	0–1.0	BB	NEE at AOD > 0.7 was greater than NEE at AOD > 0.5 and AOD < 0.35. Canopy surface temperature decreased by 0.41 °C during smoky periods.	Doughty et al. 2010
Rebio Jaru (Rondonia, Brazil)	EBF	10°04′S, 61°56′W	0–3.5	BB	No correlation between NEE and AOD. For high AOD, NEE increased as VPD decreased.	Yamasoe et al. 2006
RBJ (Rondonia, Brazil)	EBF	10°05′S, 61°55′W	0–4.0	BB	For AOD was 1.6, NEE increased by 18%, For AOD > 2.7, NEE approached zero. 50% enhancement in NEE was attributed to DFE.	Cirino et al. 2014
FLONA-Tapajós (Pará, Brazil)	EBF	3°01′S, 54°58′W	0–1.8	BB	For AOD of 1.7, NEE was enhancement by 11%. Difficult to separate the effect of temperature and humidity on NEE from radiation effects.	Oliveira et al. 2007

*Plant functional types (PFTs) include evergreen needle-leaf forest (ENF), evergreen broadleaf forest (EBF), and savanna.
†Aerosol types include urban industrial (UI) and biomass burning aerosol (BB).
‡Aerosol optical depth (AOD), net ecosystem exchange (NEE), vapor pressure deficit (VPD), and diffuse fertilization effect (DFE).

effect of aerosols was also observed in an open canopy or under low aerosol (Strada et al. 2015). For example, relatively low AOD (<0.45) does not significantly affect the savanna productivity in northern Australia (Kanniah et al. 2010). A few modeling studies have attempted to estimate the impact of aerosols on gross primary production (GPP) at regional and global scales (Mercado et al. 2009; Rap et al. 2015). Compared with no aerosols, GPP in most vegetated areas increased with the increase in diffuse radiation induced by aerosols (Chen and Zhuang 2014). Strada and Unger (2016) estimated that a 2.0% increase in global GPP was due to increased aerosols; however, Lu et al. (2017) reported a decreased GPP in the West Amazon region and Southeast Asia, which was driven by the reduction in both total and diffuse radiation due to high aerosols. Clearly, understanding the underlying mechanisms of how and at what degree the atmospheric aerosols impact terrestrial ecosystem productivity remains further to be explored.

The effects of aerosols on ecosystem productivity are physically determined by aerosol radiative perturbations (Kanniah et al. 2012; Yue and Unger 2017), which are influenced by the spatial distribution of cloudiness (Chen and Zhuang 2014; Lu et al. 2017), aerosol concentration (Lu et al. 2017), environmental conditions (Steiner and Chameides 2005; Strada and Unger 2016), and leaf area index (LAI), etc. (Lu et al. 2017; Matsui et al. 2008). Clouds and aerosols are the two most important variables that alter the quantity and quality of solar radiation (Cirino et al. 2014), albeit the effect of thick clouds on ecosystem productivity is more significant than aerosols (Cirino et al. 2014; Kanniah et al. 2012). Aerosol data, created through a cloud-screening algorithm, have been used to study the impacts of aerosols on the ecosystem to avoid the compound effects (Kanniah et al. 2012). In general, background aerosol (AOD < 0.4) has no effect on ecosystem productivity (Kanniah et al. 2010) and higher aerosol concentrations (AOD > 0.4) can lead to higher ecosystem productivity (Strada et al. 2015); however, the effects of aerosols on ecosystem productivity would change from facilitating to suppression when AOD is >2.7 (Oliveira et al. 2007). Additionally, the enhancement of ecosystem productivity by aerosols through induced DFE depends highly on the photosynthetic environmental variation (i.e., the total photosynthetically active radiation and the diffuse photosynthetically active radiation) and LAI (Yue and Unger 2017) because more leaf canopy area and more suitable environmental conditions can use light more efficiently (Kanniah et al. 2012; Lu et al. 2017).

Previous studies on aerosol impacts on ecosystem productivity and terrestrial carbon cycle are mostly centered around DFE, while the aerosol-induced perturbations on micrometeorological parameters (e.g., physical environment) are usually ignored (Niyogi et al. 2004; Strada et al. 2015; Yamasoe et al. 2006). This has led to an underestimation of the aerosol effects (Chen and Zhuang 2014; Yue and Unger 2017). Aerosols not only reduce the amount of radiation reaching the ground but also change the surface temperature and humidity (Tosca et al. 2013). After the eruption of Mt. Pinatubo in 1991, the global mean surface temperature was reduced by about 0.5 °C (Robock 2000). The cooling effect of atmospheric brown clouds may have offset 47% of surface warming by greenhouse gases, which also lead to a weaker global hydrological cycle during this period (Ramanathan and Feng 2009). Meanwhile, the aerosol-induced radiation changes can also lead to cooling and more retained water on the land surface that favors photosynthesis (Cirino et al. 2014; Doughty et al. 2010). Clearly, more studies are needed to understand how aerosols influence temperature, atmospheric humidity, canopy temperature, and ultimately their consequences on carbon absorption in different ecosystems (Steiner and Chameides 2005). Given that the effects of aerosols on terrestrial ecosystem productivity are largely dependent on the spatial and temporal changes of aerosols and aerosol radiative perturbations (Kanniah et al. 2012), an atmospheric radiative transfer module has been used to simulate solar radiation components with aerosol loading considered in regional (Rap et al. 2015) and global models (Chen and Zhuang 2014). AOD and other parameters such as the extinction angstrom exponent (EAE) and single scattering albedo (SSA) are used as drivers (O'Sullivan et al. 2016; Yue and Unger 2017). However, most studies on the aerosol effects on ecosystem productivity have only considered AOD

(Niyogi et al. 2004; Strada et al. 2015) with aerosol size and extinction ability ignored (Table 1). This leads to high uncertainties in estimating the aerosol-induced effects (Xia 2014). Aerosol type, based on aerosol size and extinction ability, is another important parameter that can cause a significant difference in aerosol effects on total and diffuse radiation (Xia 2014). For example, biomass burning aerosol (EAE $>$ 1.5, SSA $<$ 0.94) has the stronger direct effect on total radiation but a less direct effect on diffuse radiation than do urban industrial aerosol (EAE $>$ 1.5, SSA $>$ 0.94) (Xia 2014). However, there is no literature reporting the effect of aerosol types on ecosystem productivity to date.

Beijing, the capital city of China, has experienced severe haze pollution in recent decades, with AOD three times higher than that in the Washington D.C. over the same period (Keppel-Aleks and Washenfelder 2016; Yoon et al. 2016). Moreover, the aerosol optical properties in Beijing are complex due to the abundance of fine particles and complex elemental composition, which lead to a difference in total PAR and diffuse PAR (Xia 2014; Hamill et al. 2016). The complex aerosols in Beijing provide a natural laboratory to examine their impacts on ecosystem productivity. We, therefore, hypothesized that aerosol-induced perturbations in micrometeorology could increase ecosystem productivity, but significant differences exist by aerosol type. We used aerosol and micrometeorological data in combination with carbon fluxes measured by an eddy covariance system over a poplar plantation in Beijing during the 2014–2016 growing seasons (i.e., June–August) to (*i*) quantify the AOD effect on radiation and vapor pressure deficit and temperature, (*ii*) explore GPP responses to AOD and diffuse radiation, (*iii*) identify the effect of micrometeorology changes caused by aerosol disturbances on ecosystem productivity, and (*iv*) compare the effects of different aerosol types on ecosystem productivity.

2. Materials and methods

2.1. Site description

This study was carried out in a poplar plantation forest at Gongqing Forest Farm (40.01°N, 116.70°E, 29 m a.s.l.) in the northeast suburb of Beijing, China. The plantation of *Populus* × *euramericana* was planted in 1996 with 4 m × 3 m spacing with an area of 178 ha over a flat floodplain. By the end of 2016, the average canopy height was 19.52 ± 2.02 m, and the average diameter at breast height was 26.18 ± 8.52 cm. The LAI varied between 2.15 and 3.41 during the growing season of 2014–2016. The understory vegetation was dominated by *Chenopodium glaucum* L., *Artemisia annua* L., *Melilotus officinalis* (L.) Lam., and *Gaillardia aristata* Pursh.

The study site belongs to a typical subhumid warm temperature monsoon climate, with a mean annual precipitation of 576 mm. The mean annual temperature is 11.5 °C, the mean annual relative humidity is 50%, and the multiyear average of sunshine hours is 2600 h. The southeasterly winds predominate in summer and autumn. The soil texture is sandy with low water storage capacity, and the groundwater level about 2 m, which no soil moisture deficit in summer and autumn. The atmospheric environment of the study site is influenced by vehicle emissions and industrial activities in urban areas.

2.2. Eddy covariance system

An eddy covariance flux tower was installed at the center of the plantation with sufficient fetch on the upwind side of the flux tower (more details reported by Xu et al. (2017, 2018, 2020)). The sensors, including an open-path gas analyzer (EC150, Campbell Scientific Inc., CSI, Logan, Utah, USA) and a three-dimensional sonic anemometer (CSAT3, CSI), were initially installed at 26 m above the ground, and were increased to 28 m in March 2016. The radiation sensors, including a net radiometer (CNR1, Kipp and Zonen B.V., Delft, Netherlands), a pyranometer (LI-200x, LI-COR Inc., Lincoln, Nebraska, USA), and a light quantum sensor (LI-190SB, LI-COR Inc.), were installed on the top of the tower (30 m). The HC2S3 probes (CSI) were set at 0.5, 1.5, 5, 15, and 30 m above the ground to measure air temperature and relative humidity. The sensors, including thermocouples (TCAV107, CSI) and soil heat transducers (HFT3, CSI), were used to measure the soil heat fluxes at 5 and 25 cm below the soil surface. The TDR (CS616, CSI) sensors were placed at soil depths of 5, 20, 50, 100, 150, and 200 cm to measure soil moisture. All data were logged with CR3000 and CR1000 dataloggers (CSI) at 2 and 10 Hz, respectively.

2.3. Flux data processing

The flux data processing has been reported in much more detail by Xu et al. (2017, 2018). In short, using Eddypro software (LI-COR Inc.), the 10 Hz raw data were processed for 30 min mean fluxes with quality checking, spike filtering, and coordinate rotating using the planar fit method (Wilczak et al. 2001), WPL corrections (Webb et al. 1980), marginal distribution sampling (MDS), and mean diurnal variation (MDV) gap-filling method (Falge et al. 2001). The average energy balance ratio (i.e., the ratio of effective energy to available energy) was 0.90 (Xu et al. 2017), which was higher than the average value (0.84) of global flux sites (Stoy et al. 2013). Data gaps of less than 7 days were filled using the MDS approach, and gaps longer than 7 days were filled using the MDV method (Xu et al. 2018; Falge et al. 2001).

2.4. Aerosol datasets

Aerosol datasets in this study were obtained from the aerosol products of Level 2.0 provided by a measurement site located on the roof of the Institute of Atmospheric Physics Building (39.98°N, 116.38°E), Chinese Academy of Sciences in Beijing, China. This site is one of the Aerosol Robotic Network stations (AERONET, https://aeronet.gsfc.nasa.gov/). A CE318 sun/sky radiometer (Cimel, France) was used to measure the aerosol optical parameters in eight wavelengths, including 1020, 870, 500, 440, and 340 nm (Holben et al. 1998). Solar radiation measurements from multiple channels were used to calculate aerosol optical properties under the uniform algorithm (Dubovik et al. 2002; Dubovik and King 2000). The Level 2.0 data used in our study are quality-assured data, which have been cloud screened and manually quality controlled (Che et al. 2015).

2.4.1. Aerosol optical depth (AOD)

AOD is defined as the aerosol attenuation of direct beam radiation through a vertical column of the atmosphere. The CE318 sun/sky radiometer provides the AOD for each of eight bands, of which 500 nm has been widely used to represent aerosol loading (Holben et al. 1998). Hourly GPP was used to quantify the effect of AOD on the diurnal change of ecosystem productivity, and hourly AOD was differentiated into three levels following Doughty et al. (2010) and Zhang et al. (2017): background aerosol (AOD $<$ 0.4), light aerosol pollution (0.4 $\leq$ AOD $<$ 1), and severe aerosol pollution (AOD $\geq$ 1).

2.4.2. Aerosol size

The Angstrom exponent index (AE) was computed from the AOD of 440 and 870 nm to represent particle size (Dubovik et al. 2000). Fine particles ($<$2.5 μm in diameter) were abundant and dominated when AE was $>$1, and the coarse particles dominated when AE was $<$0.6. The composition ratio of fine particles to coarse particles was complex when 0.6 $\leq$ AE $\leq$ 1 (Yu et al. 2009).

$$\text{AOD}(\lambda) = \beta \lambda^{-\text{AE}} \quad (1)$$

where β is the turbidity coefficient, and λ represents wavelength.

The volume particle size distribution is one of the parameters (dV/dlnr) used to characterize the physical properties of atmospheric

aerosols. This is recorded in the range of sizes 0.05 μm ≤ r ≤ 15 μm (Holben et al. 1998).

$$\frac{dV}{d\ln r} = \frac{C_v}{\sigma\sqrt{2\pi}} \exp\left\{-\frac{1}{2}\left[\frac{\ln(r/r_v)}{\sigma}\right]^2\right\} \quad (2)$$

where dV/dlnr is the volume size distribution (μm^3·μm^{-2}), C_v is the columnar volume of particles per unit cross section of the atmospheric column, r is the particle radius, r_v is the volume geometric mean radius, and σ is the standard deviation of the natural logarithm of the radius for the volume distribution.

2.4.3. Aerosol types

The single scattering albedo (SSA) is the ratio of the scattering coefficient and the extinction coefficient (Dubovik et al. 2002).

$$SSA = \frac{\sigma_{scatt}}{\sigma_{scatt} + \sigma_{absp}} \quad (3)$$

where σ_{scatt} is the scattering coefficient, σ_{absp} is absorption coefficient, the extinction coefficient is the sum of σ_{scatt} and σ_{absp}.

The extinction Angstrom exponent (EAE) was computed as (Dubovik et al. 2002)

$$EAE = -\frac{\ln[\sigma_s(440)/\sigma_s(870)]}{\ln(440/870)} \quad (4)$$

where σ_s(440) and σ_s(870) are the extinction aerosol optical depths.

Aerosol types are classified by AOD and AE while the radiative properties of the aerosols are not characterized in the previous study (Hamill et al. 2016). In this study, single SSA and EAE were used to classify aerosol types in which each aerosol type has its own extinction and scattering properties (Giles et al. 2012; Lee et al. 2010). Dust aerosols and maritime aerosols are characterized by EAE of <0.5 (Hamill et al. 2016). Aerosols with EAE of 0.5–1.5 are classified as mixed aerosols (Hamill et al. 2016). Aerosols with EAE of >1.5 are separated into two classes based on their SSA values: urban industrial aerosols (SSA < 0.94) and biomass burning aerosols (SSA > 0.94) (Hamill et al. 2016). Moreover, the main aerosol type was in stable condition for several decades (Lee et al. 2010).

2.5. Biophysical parameters

Light-use efficiency (LUE, μmol CO_2·μmol photon^{-1}) was computed as

$$LUE = \frac{GPP}{PAR} \quad (5)$$

where GPP is gross primary productivity (μmol·m^{-2}·s^{-1}), and PAR is photosynthetically active radiation (μmol·m^{-2}·s^{-1}). The experimental site had no direct measurement of diffuse PAR. In this study, we used the Spitters model to estimate diffuse radiation and the diffuse fraction (Spitters et al. 1986).

$$k_t = \frac{s}{s_0} \quad (6)$$

$$s_0 = s_{sc}\left[1 + 0.033 \times \cos\left(\frac{360 \times t_d}{365}\right) \times \sin\theta\right] \quad (7)$$

where k_t is clearness index, s is solar radiation observed above the forest canopy, s_0 is the extraterrestrial global horizontal solar radiance, s_{sc} is the solar constant (1370 W·m^{-2}), t_d is the day of the year, and θ is the solar elevation.

When $0 < k_t < 0.3$; $\frac{s_f}{s_0} \le k_t$

$$\frac{s_f}{s_0} = k_t(1 - 0.232k_t + 0.0293\cos\theta - 6.82 \times 10^{-4}T_a + 0.0195RH) \quad (8)$$

When $0.3 < k_t < 0.78$; $0.1k_t \le \frac{s_f}{s_0} \le 0.97k_t$

$$\frac{s_f}{s_0} = k_t(1.329 - 1.1716k_t + 0.267\cos\theta - 3.67 \times 10^{-3}T_a + 0.106RH) \quad (9)$$

When $k_t > 0.78$; $\frac{s_f}{s_0} \ge 0.1k_t$

$$\frac{s_f}{s_0} = k_t(0.462k_t - 0.256\cos\theta + 3.49 \times 10^{-3}T_a + 0.0734RH) \quad (10)$$

where s_f is the diffuse solar radiation (W·m^{-2}), T_a is the air temperature (°C), RH is the relative humidity (%).

$$Fdif = \frac{[1 + 0.3 \times (1 - q^2)] \times q}{1 + (1 - q)\cos^2(90 - \theta)\cos^3\theta} \quad (11)$$

$$PAR_{dif} = PAR \times Fdif \quad (12)$$

$$PAR_{dir} = PAR - PAR_{dif} \quad (13)$$

where Fdif is the fraction of diffuse radiation, PAR_{dif} and PAR_{dir} are diffuse and direct PAR (μmol·m^{-2}·s^{-1}), respectively.

We did not have direct measurements of canopy and leaf temperature, so upward longwave emission (L, W·m^{-2}) was used to calculate the canopy temperature (Cirino et al. 2014; Doughty et al. 2010).

$$T = \left(\frac{L}{\varepsilon\sigma}\right)^{0.25} \quad (14)$$

where ε is the emissivity (0.98 for canopies) and σ is the Stefan–Boltzmann constant (5.670 × 10^{-8} W·m^{-2}·K^{-4}).

2.6. Data analysis

The relationship between ecosystem productivity and AOD was analyzed for the periods when AOD, PAR, Fdif, and GPP data were all available at midday (solar altitude angle ≥ 60°) during June–August from 2014 to 2016. The link between aerosol types and GPP was analyzed from May to September of 2014–2016. We applied a path coefficient model by focusing on the environmental factors that might be influenced by aerosols, including PAR, Fdif, VPD, and temperature, to identify the effects of AOD on GPP. All data were standardized for the models where the path coefficients were calculated based on the maximum likelihood method (Kline 2011; Saito et al. 2009). The final models were adopted when the χ^2 was non-significant, the goodness of fit index and comparative fit index were >0.9, and the root mean square error of approximation was <0.08. The path analysis was performed with AMOS software (version 24.0, IBM SPSS, Chicago, Illinois).

3. Results

3.1. Temporal changes of aerosols

There was a strong seasonal variability in AOD from 2014 to 2016, while no distinct interannual variation was observed (Fig. 1A). Overall, the AODs in the springs and summers were higher than that in the autumns and the winters, with the highest and lowest averaged monthly AOD of 1.34 ± 0.30 and 0.43 ± 0.03 in July and January, respectively. The highest daily mean AOD was 3.55, observed on 4 July 2016.

The daily average AE showed that aerosols in Beijing were dominated by fine particles (70% of daily AE was >1) (Fig. 1B). The highest daily AE (1.76) was observed on 19 June 2015. The annual average AE values were 1.11, 1.10, and 1.06 in 2014, 2015, and 2016,

Fig. 1. Change in (A) aerosol optical depth (AOD) and (B) Angstrom exponent index (AE) during 2014–2016. (A) Daily averaged AOD (500 nm); inset in panel A shows the monthly average AOD (500 nm) (A′). (B) Daily averaged AE (440–870 nm); inset in panel B shows the monthly average (440–870 nm) (B′). DOY, day of year.

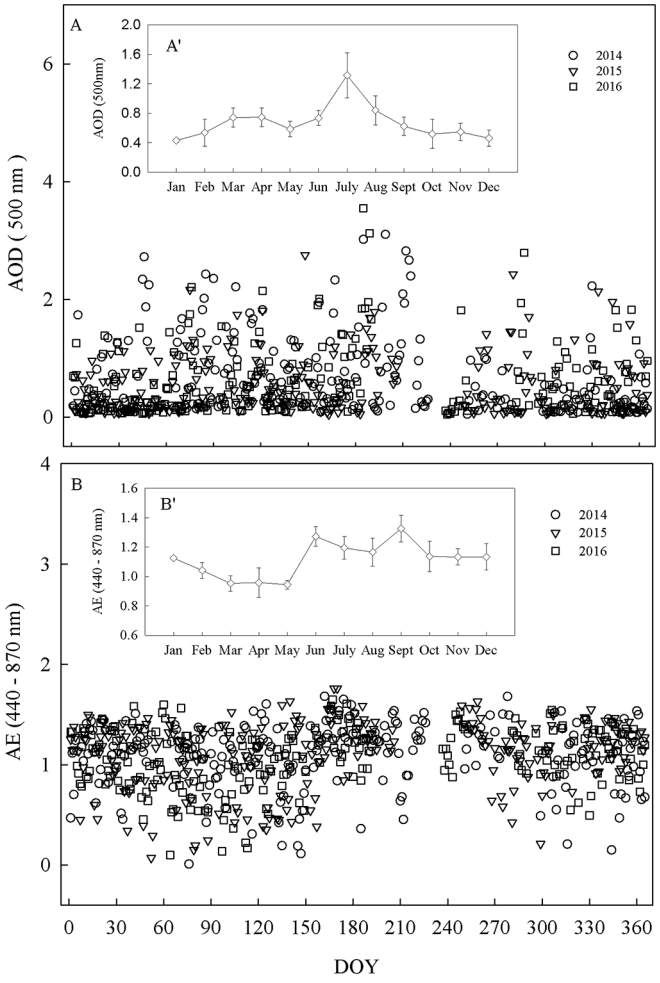

respectively, and the percentage of low AE values (AE < 0.6) was <8% during the 3 years. During June–August, the AE was larger than 1 on most days.

The frequency distribution of the hourly average AOD during 2014–2016 showed a right-skewed distribution toward the higher AOD values (Fig. 2). From June to August, 46% of the days had a AOD of <0.40. On an annual basis, 57% of the days have an AOD of <0.40. However, the percentage of days with a severe aerosol pollution (AOD ≥ 1) was 28% between June and August, which was more than the percentage of severe aerosol pollution (18%) over the entire year. The aerosol particle size distribution appeared to be bimodal from June through August (Fig. 3). The fine and coarse particles peaked at 0.1–0.3 μm and 2–5 μm, respectively. The concentration of fine particles was higher than that of coarse particles in June and July.

3.2. Aerosols effect on environmental factors

The vapor pressure deficit (VPD) was linearly correlated with the AOD (Fig. 4). As the AOD increased from 0 to 2.5, the VPD decreased by 42%, while the air temperature and canopy temperature showed no significant changes (Table 2).

Fig. 2. The frequency of aerosol optical depth (AOD) distribution. Data are shown as the count of hourly averages from 2014 to 2016.

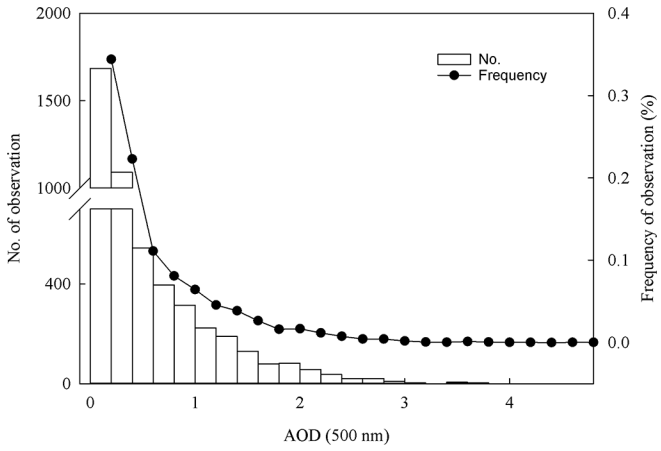

Fig. 3. Monthly averaged aerosols particle size distributions in Beijing, China, from June to August from 2014 to 2016.

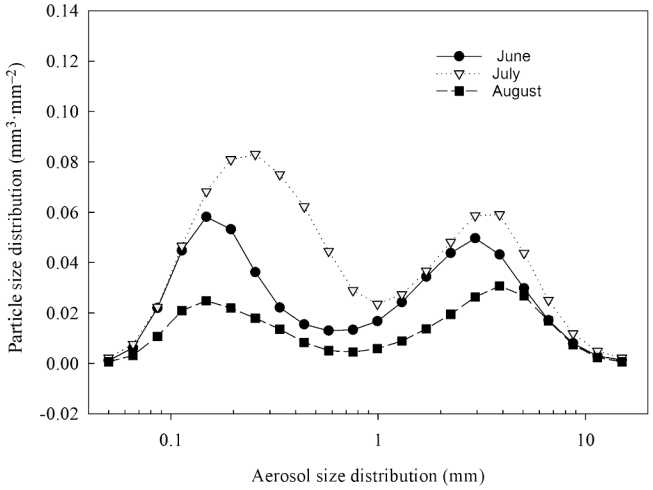

Fig. 4. Relationships between vapor pressure deficit (VPD) and aerosol optical depth (AOD). Data are shown from June to August from 2014 to 2016.

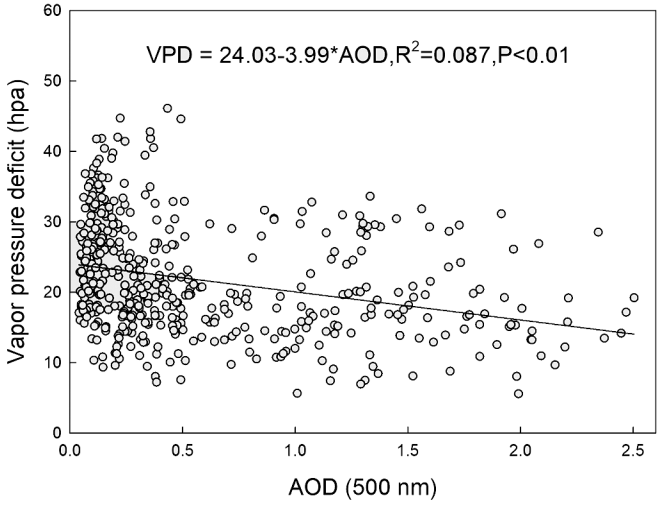

Fig. 5. Relationships between the aerosol optical depth (AOD) and (A) photosynthetically active radiation (PAR) and (B) fraction of diffuse PAR (Fdif) during June to August from 2014 to 2016 under a solar elevation of ≥60° (approximately during the period of 10:00–14:00 hours).

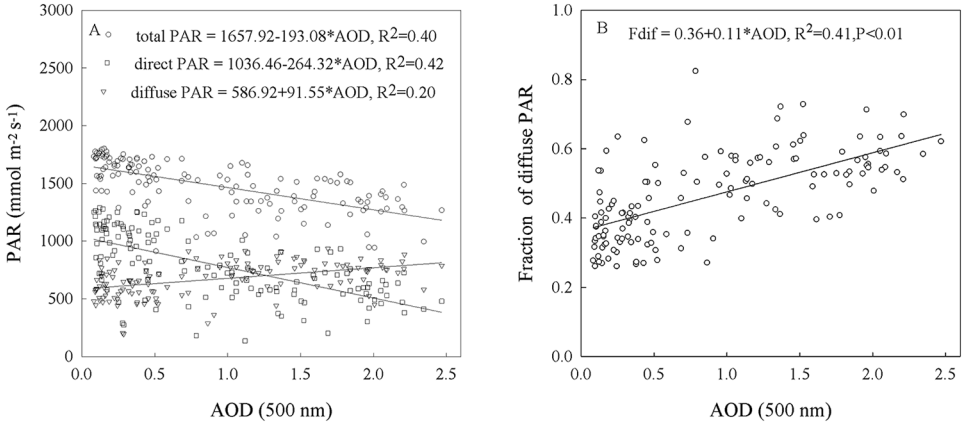

Fig. 6. Relationships between (A) light-use efficiency (LUE) and aerosol optical depth (AOD), and between (B) LUE and the diffuse fraction of photosynthetically active radiation (Fdif). Data shown are during June to August from 2014 to 2016 under the solar elevation of ≥60° (approximately during the period of 10:00–14:00 hours).

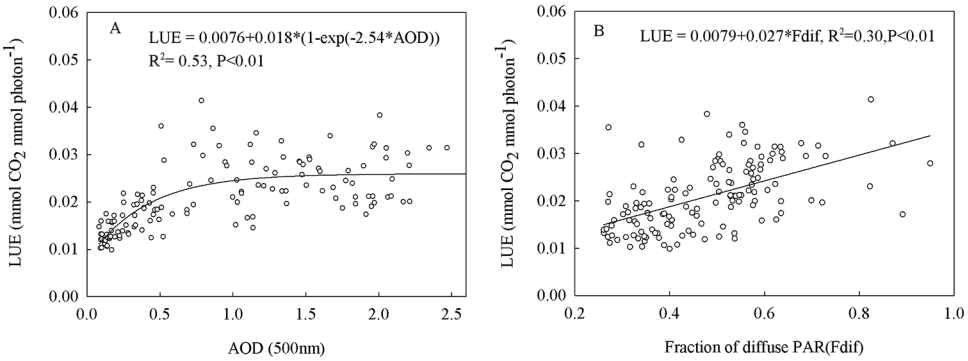

The PAR decreased while the diffuse PAR and the fraction of diffuse PAR to total PAR (Fdif) increased against AOD (Figs. 5A, 5B). The diffuse PAR increased by 228.88 μmol·m^{-2}·s^{-1} or 39%, as the AOD increased from 0 to 2.5, while the direct PAR decreased by 64%. As a result, the total PAR decreased to 29% or 482.70 μmol·m^{-2}·s^{-1} as the AOD increased from 0 to 2.5, which was coupled with a 76% increase in Fdif.

3.3. Aerosols effect on LUE and GPP

Both LUE and GPP of the ecosystem varied exponentially with AOD showing a rapid increase when AOD was <1 and almost leveled off when AOD was >1 (Figs. 6A and 7A, respectively). Meanwhile, both LUE and GPP were linearly correlated with the diffuse fraction of PAR (Fdif) (Figs. 6B and 7B, respectively). There was no significant difference in the LUE and GPP under aerosol pollutions (AOD > 0.4); however, LUE increased by 53% and 67% and GPP 36% and 37% under light aerosol pollution and severe pollution, compared with background aerosol, respectively (Table 3).

3.4. Effects of aerosols type on LUE and GPP

Mixed aerosol was the main aerosol type in Beijing (86% of all aerosols) during the study period (Fig. 8). Dust, biomass burning, and urban industrial aerosols accounted for 7%, 3%, and 4%, respectively. Maritime aerosol was not the main aerosol type for any day during the study period.

There were significant differences in the AOD and LUE under different aerosol types (Table 4). The highest AOD and LUE were detected under the urban industrial type, but the highest Fdif were found under the mixed aerosol type.

Table 2. Effect of aerosols on air and canopy temperatures at solar elevation angle of ≥60° during June–August from 2014 to 2016.

Aerosol level	AOD (500 nm)	Air temp. (°C)	Canopy temp. (°C)
Background aerosol	0.16a ± 0.10	29.24a ± 1.53	30.01a ± 2.23
Light aerosol pollution	0.62b ± 0.23	29.92a ± 1.79	30.56a ± 2.27
Severe aerosol pollution	1.68c ± 0.38	30.05a ± 1.90	30.40a ± 2.51

Note: Hourly AOD was differentiated into three levels: background aerosol (AOD < 0.4), light aerosol pollution (0.4 ≤ AOD < 1), and severe aerosol pollution (AOD ≥ 1). Data are presented as mean ± SE; different lowercase letters indicate significant differences among the means ($p < 0.05$).

4. Discussion

4.1. The diffuse fertilization of aerosols on ecosystem productivity

Our results showed that the GPP of the poplar plantation did increase as the AOD increased under background aerosol and light aerosol pollution (Fig. 7A); however, aerosols had no significant effect on the GPP as under severe aerosol pollution (Fig. 7A; Table 3). Yue and Unger (2017) reported that aerosol pollution lead only weak facilitation of the net primary production in the North China Plain, which is similar to our findings in Beijing. In general, sunlit leaves received both direct and diffuse PAR, which

Table 3. The effect of aerosols on photosynthetically active radiation (PAR), the diffuse fraction of PAR (Fdif), light-use efficiency (LUE), and gross primary productivity (GPP).

Aerosol level	PAR ($\mu mol \cdot m^{-2} \cdot s^{-1}$)	Fdif	LUE ($\mu mol\ CO_2 \cdot \mu mol\ photon^{-1}$)	GPP ($\mu mol \cdot m^{-2} \cdot s^{-1}$)
Background aerosol	1641.65a ± 155.51	0.38a ± 0.11	0.015a ± 0.0033	24.01a ± 4.81
Light aerosol pollution	1566.48a ± 214.62	0.45a ± 0.14	0.023b ± 0.0069	32.63b ± 7.41
Severe aerosol pollution	1344.51a ± 176.26	0.57b ± 0.11	0.025b ± 0.0053	32.86b ± 5.88

Note: Hourly AOD was differentiated into three levels: background aerosol (AOD < 0.4), light aerosol pollution (0.4 ≤ AOD < 1), and severe aerosol pollution (AOD ≥ 1). Data are presented as mean ± SE; different lowercase letters indicate significant differences among the means ($p < 0.05$).

Table 4. The effect of aerosol type on photosynthetically active radiation (PAR), the diffuse fraction of PAR (Fdif), light-use efficiency (LUE) and gross primary productivity (GPP) in daytime during May–September from 2014 to 2016.

Aerosol type	AOD (500 nm)	PAR ($\mu mol \cdot m^{-2} \cdot s^{-1}$)	Fdif	LUE ($\mu mol\ CO_2 \cdot \mu mol\ photon^{-1}$)	GPP ($\mu mol \cdot m^{-2} \cdot s^{-1}$)
Biomass burning	0.56 ± 0.15	558.95b ± 430.79	0.47a ± 0.32	0.025a ± 0.007	19.09a ± 3.82
Urban industrial	0.96 ± 0.30	393.13a ± 270.65	0.43a ± 0.09	0.041b ± 0.016	18.88a ± 3.35
Mixed aerosol	0.83 ± 0.45	511.40b ± 302.81	0.55b ± 0.19	0.034b ± 0.011	20.12a ± 6.95

Note: Aerosol types are determined based on extinction angstrom exponent (EAE) (440–870 nm) and single scattering albedo (SSA) (440 nm) — biomass burning (EAE > 1.5, SSA < 0.94), urban industrial (EAE > 1.5, SSA > 0.94), mixed aerosol (0.5 < EAE < 1.5). Data are presented as mean ± SE; different lowercase letters indicate significant differences among the means ($p < 0.05$).

Fig. 7. Relationships between (A) gross primary productivity (GPP) and aerosol optical depth (AOD) and between (B) GPP and the diffuse fraction of photosynthetically active radiation (PAR). Data shown are during June to August from 2014 to 2016 under the solar elevation of ≥60° (approximately during the period of 10:00–14:00 hours).

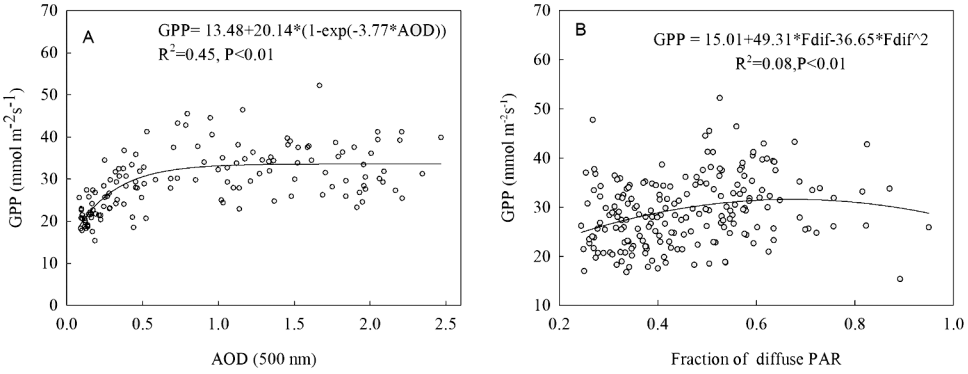

Fig. 8. Schematic illustration of aerosol classification based on extinction angstrom exponent (440–870 nm) and single scattering albedo (440 nm) in Beijing, China, for 2014–2016.

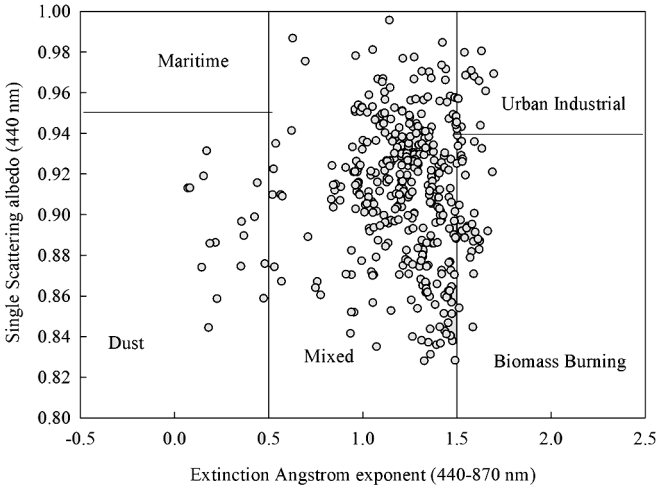

are abundant under sunny, summer days, but shaded leaves received only diffuse PAR, which are usually light-limited (Gu et al. 2002). Aerosol radiative perturbations can increase the diffuse PAR and diffused blue wavelengths, which in turn can not only reduce the light saturation of sunlit leaves but also increase the photosynthesis of shaded leaves (Kanniah et al. 2010, 2012). Therefore, both sunlit and shaded leaves can be benefited from the aerosol DFE (Strada et al. 2015; Yue and Unger 2017).

Ecosystem productivity of most forests would increase due to aerosol DFE (e.g., enhanced LUE) under light aerosol pollution, but a few ecosystems may decrease their productivity when there is a reduction in total radiation that cannot be compensated by the DFE for forests under high aerosol condition (AOD > 3) (Chen and Zhuang 2014; Cirino et al. 2014; Oliveira et al. 2007). In West Amazonia, ecosystem productivity decreased when AOD exceeds 3 or Fdif increased to 0.8 (Cirino et al. 2014). In our study, when the AOD increased from 1 to 2.5, the total PAR decreased by 15%, the aerosol DFE offset the reduction of the poplar ecosystem productivity caused by the total radiation decrease, while the GPP remained at a high level when the Fdif was 0.47–0.76 (Fig. 7B). Moreover, the aerosol DFE was also sensitive to canopy structure (Yue and Unger 2017). The aerosol DFE on ecosystem productivity is either neutral or negative for grassland or shrub wood

Fig. 9. The effects of aerosol optical depth (AOD) on gross primary productivity (GPP) under aerosol pollution. VPD, vapor pressure deficit; PAR, photosynthetically active radiation; Fdif, diffuse fraction of PAR; GPP, gross primary productivity. The χ^2 was 0.06, the goodness of fit index was 0.97, comparative fit index was 0.97, and the root mean square error was 0.78. The value on each path is standardized path coefficients (–1 to 1), where $p < 0$ denotes negative correlation and $p > 0$ denotes positive correlation. Data are shown under the solar elevation of ≥60° (approximately during the period of 10:00–14:00 hours).

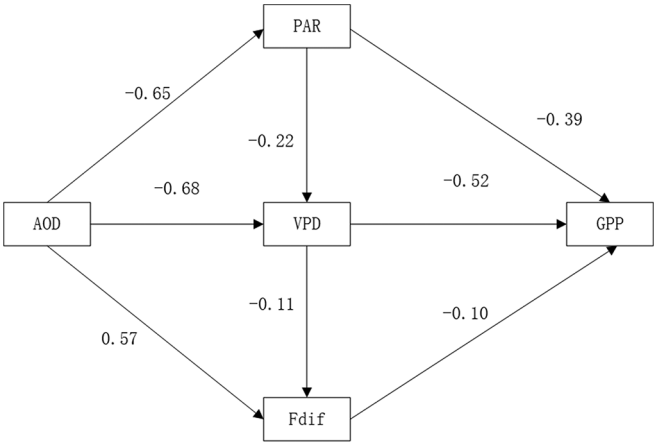

environments (Chen and Zhuang 2014; Kanniah et al. 2012). Therefore, forest ecosystems are more likely to see increased ecosystem productivity due to DFE under light aerosol pollution conditions.

4.2. Effect of aerosol-perturbed micrometeorological changes on the productivity

Air temperature may increase due to the atmospheric boundary layer responding to longwave radiation during the nighttime and winter; this cooling effect of aerosols has been more strongly observed in daytime and summer (Huang et al. 2007). In our study, aerosols showed no significant cooling effect on the air temperature and canopy temperature at noon (Table 2), which was consistent with previous research that aerosols are not significantly correlated to the air temperature. However, using a regional climate-terrestrial biosphere model to simulate aerosol impacts on terrestrial photosynthesis, Steiner and Chameides (2005) concluded that diurnally averaged leaf temperature decreased by ∼3 °C at noon and the temperature differences between the leaf temperature and the air temperature is as high as 6 °C under the influence of the aerosols in the Yellow River region. Previous studies have also shown that the diffuse radiation is much more efficient than direct radiation for assimilation and there is even no saturation under the high diffuse radiation (Gu et al. 2002; Moffat et al. 2010). If the diffuse radiation is not included, ecosystem productivity could be underestimated (Cohan et al. 2002; Mercado et al. 2009), or the effect of the aerosols on micrometeorological conditions is overestimated (Gu et al. 2002; Wohlfahrt et al. 2008). Moreover, canopy (leaf) temperature was reported to be strongly correlated with the air temperature, but an uncoupling occurred during a dry season when PAR varied greatly (Sanchez et al. 2018). In addition, the difference between the canopy temperature and air temperature was not significant (Table 2). Similar results were also observed within an Amazon tropical forest (Doughty et al. 2010). Our path analysis showed that aerosols had a positive effect on GPP by perturbing micrometeorological factors under severe aerosol pollution, and the aerosols did create a wetter environment due to decreased evaporation as a result of the increased vapor pressure and the decreased VPD (Fig. 4). Sunlit leaves often exceed the optimum for photosynthesis during midday under clear-sky conditions in the summer, which may cause photodamage when plants are under water stress (Zhou et al. 2007). The effect of the aerosols on micrometeorological factors (e.g., temperature and VPD) can reduce water stress and heat stress and thereby improve sunlit leaf photosynthesis (Cirino et al. 2014; Huang et al. 2007). Therefore, aerosols indirectly influence thermal and hydrologic conditions to favor the photosynthetic processes of ecosystems.

Our path analysis suggested that the aerosols, radiation, and VPD jointly influenced GPP (Fig. 9). However, Doughty et al. (2010) estimated that the increase in productivity with an increase in aerosols was about 20% due to the change of temperature and about 80% due to increased subcanopy diffuse radiation. Cirino et al. (2014) concluded that a 50% increase of ecosystem productivity was attributed to an increase in Fdif. In our study, aerosols reduced total radiation and thus affected the VPD, and VPD in turn affected diffuse radiation and diffuse fraction (Fig. 9). Similarly, Wohlfahrt et al. (2008) found that changes in air temperature and humidity amplified the diffuse radiation effect in a temperate mountain grassland ecosystem. Therefore, the effect of aerosol on ecosystem productivity cannot completely distinguish whether the enhancements are caused by DFE or by the aerosol on micrometeorological factors.

4.3. The effect of aerosol type on ecosystem productivity

The aerosol concentration, aerosol optical properties, and aerosol types are important regulators on aerosol radiation (Xia 2014). However, the AOD of different aerosols types are highly uncertain, as they are derived from different emission sources (Hamill et al. 2016). In our study, the high AOD (Fig. 1), fine particles, and high secondary pollution (Fig. 3) were the main characteristics of Beijing aerosols during June–August, which formed different optical properties, and thus were mainly assigned to the mixed aerosol type (Hamill et al. 2016). Several studies have shown that active photochemical reactions and fine particle pollution with strong scattering effects were severe in summer in Beijing (Li et al. 2012; Qian et al. 2006). The fine particulate matter was therefore responsible for increasing diffuse PAR and even local dimming in the last 10 years (Alpert et al. 2005; Wild et al. 2005).

Aerosol radiative perturbations varied with aerosol types (Xia 2014). Absorbing aerosols had the largest aerosol direct radiative effect on total radiation, but scattering aerosols had a larger radiative effect on diffuse radiation than that of absorbing aerosol (Xia 2014). García et al. (2012) found that absorbing aerosols from biomass burning has the greatest impact on total radiation at the bottom of the atmosphere. Moreover, the scattering aerosol with high SSA was more likely to increase latent heat and promote photosynthesis (Murthy et al. 2014). In our study, we found that the effect of mixed aerosols on GPP was much more efficient than that of urban industrial and biomass burning aerosols (Table 5). Hamill et al. (2016) found that mixed aerosols in Beijing had better scattering abilities compared with urban industrial aerosols (with weak absorption) and biomass burning aerosols (with weak scattering). The mixed aerosols with higher Fdif had a stronger aerosol DFE, which could be the reason that the regression slope of GPP against aerosol in our study was larger than that in other regions (Table 5). Therefore, aerosol type is a factor for evaluating the aerosol impacts on ecosystem productivity and terrestrial carbon sink.

Atmospheric aerosols and clouds are two important variables that influence solar radiation, the micrometeorological environment, and thus ecosystem photosynthesis (Oliveira et al. 2007; Cirino et al. 2014). The atmospheric aerosols elevated the ecosystem productivity of a poplar plantation in northern China due to the aerosol-induced changes in PAR and other environmental factors at midday under clear sky conditions (AOD < 2.5). However,

Table 5. The effect of aerosol type on forest ecosystem productivity.

Aerosol type	Site	Factor (slope)	Reference
Biomass burning	K34	4.33	Cirino et al. 2014
	Ji-Parana	2.75	Cirino et al. 2014
	FLONA-Tapajós	1.51	Oliveira et al. 2007
	RBJ	1.85	Oliveira et al. 2007
	Rebio Jaru	3.33	Yamasoe et al. 2006
Mean		**2.75 ± 1.14**	
Urban industrial	Harvard Forest	5.20	Strada et al. 2015
	Park Falls	3.75	Strada et al. 2015
	Willow Creek	4.61	Strada et al. 2015
	SMEAR Estonia	6.85	Ezhova et al. 2018
Mean		**5.10 ± 1.31**	
Mixed aerosol	Shunyi Poplar	8.06	Our result

Note: The factors are the regression slopes between forest ecosystem productivity and aerosol optical depth (AOD). If AOD was large enough to decrease ecosystem productivity, the regression slope was calculated corresponding to the optimal aerosol fertilization effect. Aerosol types are determined based on extinction angstrom exponent (EAE) (440–870 nm) and single scattering albedo (SSA) (440 nm) — biomass burning (EAE > 1.5, SSA < 0.94), urban industrial (EAE > 1.5, SSA > 0.94), mixed aerosol (0.5 < EAE < 1.5).

whether aerosols could promote GPP at different solar altitude angles has not been analyzed. The combined effects of aerosol and cloud on GPP would need to be explored in conjunction with observational data and ecosystem models as soon as possible.

5. Conclusions

We found that aerosol can increase the GPP of the plantation by 37% under severe aerosol pollution compared with background aerosols. Aerosol-induced perturbations in micrometeorological parameters increased ecosystem productivity by decreasing 40% VPD. The difference in the effect of aerosol type on ecosystem productivity between the three aerosol types suggested that the mixed aerosol type had a stronger effect on the ecosystem GPP than did the urban industrial aerosol and biomass burning aerosols. The aerosol DFE and the aerosol-induced perturbations in micrometeorological parameters jointly contributed to elevated ecosystem productivity of a poplar plantation. Thus, further studies focusing on the effect of aerosol on ecosystem productivity by modeling so as to better predict ecosystem productivity under the background of climate change.

Acknowledgements

This study was financially supported by National Science Foundation of China through the project "Impact mechanism of atmospheric aerosols on forest ecosystem carbon and water coupling" (grant 31872711) and the Beijing Municipal Education Commission through Innovative Transdisciplinary Program of Ecological Restoration Engineering. Concerning the AERONET data used in this paper, we are particularly grateful to Hongbin Chen and Philippe Goloub for their efforts in establishing and maintaining the Beijing site and their assistants for the upkeep of the instrumentation and availability of the online data.

References

Alpert, P., Kishcha, P., Kaufman, Y.J., and Schwarzbard, R. 2005. Global dimming or local dimming: effect of urbanization on sunlight availability. Geophys. Res. Lett. **32**: L17802. doi:10.1029/2005GL023320.

Alton, P.B. 2008. Reduced carbon sequestration in terrestrial ecosystems under overcast skies compared to clear skies. Agric. For. Meteorol. **148**(10): 1641–1653. doi:10.1016/j.agrformet.2008.05.014.

Alton, P.B., North, P.R., and Los, S.O. 2007. The impact of diffuse sunlight on canopy light-use efficiency, gross photosynthetic product and net ecosystem exchange in three forest biomes. Glob. Change Biol. **13**(4): 776–787. doi:10.1111/j.1365-2486.2007.01316.x.

Che, H., Xia, X.G., Zhu, J., Wang, H., Wang, Y.Q., Sun, J.Y., et al. 2015. Aerosol optical properties under the condition of heavy haze over an urban site of Beijing, China. Environ. Sci. Pollut. Res. **22**(2): 1043–1053. doi:10.1007/s11356-014-3415-5.

Chen, M., and Zhuang, Q. 2014. Evaluating aerosol direct radiative effects on global terrestrial ecosystem carbon dynamics from 2003 to 2010. Tellus B Chem. Phys. Meteorol. **66**: 21808. doi:10.3402/tellusb.v66.21808.

Cirino, G.G., Souza, R.A.F., Adams, D.K., and Artaxo, P. 2014. The effect of atmospheric aerosol particles and clouds on net ecosystem exchange in the Amazon. Atmos. Chem. Phys. **14**(13): 6523–6543. doi:10.5194/acp-14-6523-2014.

Cohan, D.S., Xu, J., Greenwald, R., Bergin, M.H., and Chameides, W.L. 2002. Impact of atmospheric aerosol light scattering and absorption on terrestrial net primary productivity. Global Biogeochem. Cycles, **16**(4): 37-1–37-12. doi:10.1029/2001GB001441.

Doughty, C.E., Flanner, M.G., and Goulden, M.L. 2010. Effect of smoke on subcanopy shaded light, canopy temperature, and carbon dioxide uptake in an Amazon rainforest. Global Biogeochem. Cycles, **24**(3): GB3015. doi:10.1029/2009GB003670.

Dubovik, O., and King, M.D. 2000. A flexible inversion algorithm for retrieval of aerosol optical properties from sun and sky radiance measurements. J. Geophys. Res. **105**: 20673–20696. doi:10.1029/2000JD900282.

Dubovik, O., Smirnov, L.A., Holben, B.N., King, M.D., Kaufman, Y.J., Eck, T.F., and Slutsker, I. 2000. Accuracy assessments of aerosol optical properties retrieved from Aerosol Robotic Network (AERONET) sun and sky radiance measurements. J. Geophys. Res. **105**: 9791–9806. doi:10.1029/2000JD900040.

Dubovik, O., Holben, B.N., Eck, T.F., Smirnov, A., Kaufman, Y.J., King, M.D., et al. 2002. Variability of absorption and optical properties of key aerosol types observed in worldwide locations. J. Atmos. Sci. **59**(3): 590–608. doi:10.1175/1520-0469(2002)059<0590:VOAAOP>2.0.CO;2.

Ezhova, E., Ylivinkka, I., Kuusk, J., Komsaare, K., Vana, M., Krasnova, A., et al. 2018. Direct effect of aerosols on solar radiation and gross primary production in boreal and hemiboreal forests. Atmos. Chem. Phys. **18**(24): 17863–17881. doi:10.5194/acp-18-17863-2018.

Falge, E., Baldocchi, D.D., Olson, R., Anthoni, P.M., Aubinet, M., Bernhofer, C., et al. 2001. Gap filling strategies for defensible annual sums of net ecosystem exchange. Agric. For. Meteorol. **107**(1): 43–69. doi:10.1016/S0168-1923(00)00225-2.

García, O.E., Díaz, J.P., Expósito, F.J., Díaz, A.M., Dubovik, O., Derimian, Y., et al. 2012. Shortwave radiative forcing and efficiency of key aerosol types using AERONET data. Atmos. Chem. Phys. **12**(11): 5129–5145. doi:10.5194/acp-12-5129-2012.

Giles, D.M., Holben, B.N., Eck, T.T., Sinyuk, A., Smirnov, A., Slutsker, I., et al. 2012. An analysis of AERONET aerosol absorption properties and classifications representative of aerosol source regions. J. Geophys. Res. **117**: D17203. doi:10.1029/2012JD018127.

Gu, L.H., Baldocchi, D.D., Verma, S.B., Black, T.A., Vesala, T., Falge, E., and Dowty, P.R. 2002. Advantages of diffuse radiation for terrestrial ecosystem productivity. J. Geophys. Res. **107**: ACL 2-1–ACL 2-23. doi:10.1029/2001JD001242.

Gu, L.H., Baldocchi, D.D., Wofsy, S.C., Munger, J.W., Michalsky, J.J., Urbanski, S.P., and Boden, T.A. 2003. Response of a deciduous forest to the Mount Pinatubo eruption: enhanced photosynthesis. Science, **299**(5615): 2035–2038. doi:10.1126/science.1078366. PMID:12663919.

Hamill, P., Giordano, M., Ward, C., Giles, D., and Holben, B. 2016. An AERONET-based aerosol classification using the Mahalanobis distance. Atmos. Environ. **140**: 213–233. doi:10.1016/j.atmosenv.2016.06.002.

Holben, B.N., Eck, T.F., Slutsker, I., Tanre, D., Buis, J., Setzer, A., et al. 1998. AERONET: a federated instrument network and data archive for aerosol characterization. Remote Sens. Environ. **66**(1): 1–16. doi:10.1016/S0034-4257(98)00031-5.

Huang, Y., Chameides, W.L., and Dickinson, R.E. 2007. Direct and indirect effects of anthropogenic aerosols on regional precipitation over East Asia. J. Geophys. Res. **112**: D0312. doi:10.1029/2006JD007114.

Kanniah, K.D., Beringer, J., Tapper, N.J., and Long, C.N. 2010. Aerosols and their influence on radiation partitioning and savanna productivity in northern Australia. Theor. Appl. Climatol. **100**(3–4): 423–438. doi:10.1007/s00704-009-0192-z.

Kanniah, K.D., Beringer, J., North, P., and Hutley, L. 2012. Control of atmospheric particles on diffuse radiation and terrestrial plant productivity: a review. Prog. Phys. Geogr. Earth Environ. **36**(2): 209–237. doi:10.1177/0309133311434244.

Keppel-Aleks, G., and Washenfelder, R.A. 2016. The effect of atmospheric sulfate reductions on diffuse radiation and photosynthesis in the United States during 1995–2013. Geophys. Res. Lett. **43**(18): 9984–9993. doi:10.1002/2016GL070052.

Kline, B. 2011. Principles and practice of structural equation modeling. The Guildford Press, New York.

Lee, J., Kim, J., Song, C.H., Kim, S.B., Chun, Y., Sohn, B., and Holben, B.N. 2010. Characteristics of aerosol types from AERONET sunphotometer measurements. Atmos. Environ. **44**(26): 3110–3117. doi:10.1016/j.atmosenv.2010.05.035.

Li, B., Su, S., Yuan, H., and Tao, S. 2012. Spatial and temporal variations of AOD over land at the global scale. Int. J. Remote Sens. **33**(7): 2097–2111. doi:10.1080/01431161.2011.605088.

Lu, X., Chen, M., Liu, Y., Miralles, D.G., and Wang, F. 2017. Enhanced water use efficiency in global terrestrial ecosystems under increasing aerosol loadings. Agric. For. Meteorol. **237–238**: 39–49. doi:10.1016/j.agrformet.2017.02.002.

Matsui, T., Beltrán-Przekurat, A., Niyogi, D., Pielke, R.A., and Coughenour, M. 2008. Aerosol light scattering effect on terrestrial plant productivity and energy fluxes over the eastern United States. J. Geophys. Res. **113**: D14S14. doi:10.1029/2007JD009658.

Mercado, L.M., Bellouin, N., Sitch, S., Boucher, O., Huntingford, C., Wild, M., and Cox, P.M. 2009. Impact of changes in diffuse radiation on the global land carbon sink. Nature, **458**(7241): 1014–1017. doi:10.1038/nature07949. PMID:19396143.

Misson, L., Lunden, M., McKay, M., and Goldstein, A.H. 2005. Atmospheric aerosol light scattering and surface wetness influence the diurnal pattern of net ecosystem exchange in a semi-arid ponderosa pine plantation. Agric. For. Meteorol. **129**(1–2): 69–83. doi:10.1016/j.agrformet.2004.11.008.

Moffat, A.M., Beckstein, C., Churkina, G., Mund, M., and Heimann, M. 2010. Characterization of ecosystem responses to climatic controls using artificial neural networks. Glob Chang Biol. **16**(10): 2737–2749. doi:10.1111/j.1365-2486.2010.02171.x.

Murthy, B.S., Latha, R., Kumar, M., and Mahanti, N.C. 2014. Effect of aerosols on evapo-transpiration. Atmos. Environ. **89**: 109–118. doi:10.1016/j.atmosenv.2014.02.029.

Niyogi, D., Chang, H., Saxena, V.K., Holt, T., Alapaty, K., Booker, F.L., et al. 2004. Direct observations of the effects of aerosol loading on net ecosystem CO_2 exchanges over different landscapes. Geophys. Res. Lett. **31**: L20506. doi:10.1029/2004GL020915.

Oliveira, P.H., Artaxo, P., Pires, C., Lucca, S.D., Procopio, A.S., Holben, B.N., et al. 2007. The effects of biomass burning aerosols and clouds on the CO_2 flux in Amazonia. Tellus B Chem. Phys. Meteorol. **59**(3): 338–349. doi:10.1111/j.1600-0889.2007.00270.x.

O'Sullivan, M., Rap, A., Reddington, C.L., Spracklen, D.V., Gloor, M., and Buermann, W. 2016. Small global effect on terrestrial net primary production due to increased fossil fuel aerosol emissions from East Asia since the turn of the century. Geophys. Res. Lett. **43**(15): 8060–8067. doi:10.1002/2016GL068965. PMID:27773953.

Qian, Y., Kaiser, D.P., Leung, L.R., and Xu, M. 2006. More frequent cloud-free sky and less surface solar radiation in China from 1955 to 2000. Geophys. Res. Lett. **33**: L01812. doi:10.1029/2005GL024586.

Ramanathan, V., and Feng, Y. 2009. Air pollution, greenhouse gases and climate change: global and regional perspectives. Atmos. Environ. **43**(1): 37–50. doi:10.1016/j.atmosenv.2008.09.063.

Rap, A., Spracklen, D.V., Mercado, L.M., Reddington, C.L., Haywood, J.M., Ellis, R., et al. 2015. Fires increase Amazon forest productivity through increases in diffuse radiation. Geophys. Res. Lett. **42**(11): 4654–4662. doi:10.1002/2015GL063719.

Robock, A. 2000. Volcanic eruptions and climate. Rev. Geophys. **38**(2): 191–219. doi:10.1029/1998RG000054.

Saito, M., Kato, T., and Tang, Y.H. 2009. Temperature controls ecosystem CO_2 exchange of an alpine meadow on the northeastern Tibetan Plateau. Glob Chang Biol. **15**(1): 221–228. doi:10.1111/j.1365-2486.2008.01713.x.

Sanchez, A., Rey-Sánchez, A.C., Posada, J.M., and Smith, W.K. 2018. Interplay of seasonal sunlight, air and leaf temperature in two alpine páramo species, Colombian Andes. Agric. For. Meteorol. **253–254**: 38–47. doi:10.1016/j.agrformet.2018.01.033.

Spitters, C.J.T., Toussaint, H.A.J.M., and Goudriaan, J. 1986. Separating the diffuse and direct component of global radiation and its implications for modeling canopy photosynthesis Part I. Components of incoming radiation. Agric. For. Meteorol. **38**(1): 217–229. doi:10.1016/0168-1923(86)90060-2.

Steiner, A.L., and Chameides, W.L. 2005. Aerosol-induced thermal effects increase modelled terrestrial photosynthesis and transpiration. Tellus B Chem. Phys. Meteorol. **57**: 404–411. doi:10.3402/tellusb.v57i5.16559.

Stoy, P.C., Mauder, M., Foken, T., Marcolla, B., Boegh, E., Ibrom, A., et al. 2013. A data-driven analysis of energy balance closure across FLUXNET research sites: the role of landscape scale heterogeneity. Agric. For. Meteorol. **171–172**: 137–152. doi:10.1016/j.agrformet.2012.11.004.

Strada, S., and Unger, N. 2016. Potential sensitivity of photosynthesis and isoprene emission to direct radiative effects of atmospheric aerosol pollution. Atmos. Chem. Phys. **16**(7): 4213–4234. doi:10.5194/acp-16-4213-2016.

Strada, S., Unger, N., and Yue, X. 2015. Observed aerosol-induced radiative effect on plant productivity in the eastern United States. Atmos. Environ. **122**: 463–476. doi:10.1016/j.atmosenv.2015.09.051.

Tosca, M.G., Randerson, J.T., and Zender, C.S. 2013. Global impact of smoke aerosols from landscape fires on climate and the Hadley circulation. Atmos. Chem. Phys. **13**: 5227–5241. doi:10.5194/acp-13-5227-2013.

Webb, E., Pearman, G.I., and Leuning, R. 1980. Correction of flux measurements for density effects due to heat and water vapour transfer. Q. J. R. Meteorol. Soc. **106**: 85–100. doi:10.1002/qj.49710644707.

Wilczak, M., Oncley, S.P., and Stage, A. 2001. Sonic anemometer tilt correction algorithms. Boundary-Layer Meteorol. **99**(1): 127–150. doi:10.1023/A:1018966204465.

Wild, M., Gilgen, H., Gilgen, H., Roesch, A., Ohmura, A., Long, C.N., et al. 2005. From dimming to brightening: decadal changes in solar radiation at Earth's surface. Science, **308**(5723): 847–850. doi:10.1126/science.1103215. PMID:15879214.

Wohlfahrt, G., Wohlfahrt, G., Hammerle, A., Haslwanter, A., Bahn, M., Tappeiner, U., and Cernusca, A. 2008. Disentangling leaf area and environmental effects on the response of the net ecosystem CO_2 exchange to diffuse radiation. Geophys. Res. Lett. **35**(16): L16805. doi:10.1029/2008GL035090. PMID:24347740.

Xia, X. 2014. A critical assessment of direct radiative effects of different aerosol types on surface global radiation and its components. J. Quant. Spectrosc. Radiat Transfer, **149**: 72–80. doi:10.1016/j.jqsrt.2014.07.020.

Xu, H., Zhang, Z., Chen, J., Zhu, M., and Kang, M. 2017. Cloudiness regulates gross primary productivity of a poplar plantation under different environmental conditions. Can. J. For. Res. **47**(5): 648–658. doi:10.1139/cjfr-2016-0413.

Xu, H., Zhang, Z.Q., Chen, J.Q., Xiao, J.F., Zhu, M.X., Kang, M.C., and Cao, W.X. 2018. Regulations of cloudiness on energy partitioning and water use strategy in a riparian poplar plantation. Agric. For. Meteorol. **262**: 135–146. doi:10.1016/j.agrformet.2018.07.008.

Xu, H., Zhang, Z., Xiao, J., Chen, J., Zhu, M., Cao, W., and Chen, Z. 2020. Environmental and canopy stomatal control on ecosystem water use efficiency in a riparian poplar plantation. Agric. For. Meteorol. **287**: 107953. doi:10.1016/j.agrformet.2020.107953.

Yamasoe, M.A., van Randow, C., Manzi, A.O., Schafer, J.S., Eck, T.F., and Holben, B.N. 2006. Effect of smoke and clouds on the transmissivity of photosynthetically active radiation inside the canopy. Atmos. Chem. Phys. **6**: 1645–1656. doi:10.5194/acp-6-1645-2006.

Yoon, J., Pozzer, A., Chang, D.Y., Lelieveld, J., Kim, J., Kim, M., et al. 2016. Trend estimates of AERONET-observed and model-simulated AOTs between 1993 and 2013. Atmos. Environ. **125**: 33–47. doi:10.1016/j.atmosenv.2015.10.058.

Yu, X., Zhu, B., and Zhang, M. 2009. Seasonal variability of aerosol optical properties over Beijing. Atmos. Environ. **43**(26): 4095–4101. doi:10.1016/j.atmosenv.2009.03.061.

Yue, X., and Unger, N. 2017. Aerosol optical depth thresholds as a tool to assess diffuse radiation fertilization of the land carbon uptake in China. Atmos. Chem. Phys. **17**(2): 1329–1342. doi:10.5194/acp-17-1329-2017.

Zhang, M., Ma, Y.Y., Gong, W., Wang, L.C., Xia, X.A., Che, H.Z., et al. 2017. Aerosol radiative effect in UV, VIS, NIR, and SW spectra under haze and high-humidity urban conditions. Atmos. Environ. **166**: 9–21. doi:10.1016/j.atmosenv.2017.07.006.

Zhou, Y., Lam, H.M., and Zhang, J. 2007. Inhibition of photosynthesis and energy dissipation induced by water and high light stresses in rice. J. Exp. Bot. **58**(5): 1207–1217. doi:10.1093/jxb/erl291. PMID:17283375.